

## Quantitative structural analysis of organic thin films: An x-ray diffraction study

Casey W. Miller, A. Sharoni, G. Liu, C. N. Colesniuc, B. Fruhberger, and Ivan K. Schuller  
*Department of Physics, University of California, San Diego, 9500 Gilman Drive, La Jolla, California 92093, USA*  
 (Received 13 May 2005; revised manuscript received 5 August 2005; published 28 September 2005)

The SUPREX thin film refinement of x-ray diffraction (XRD) was used to quantitatively analyze the structure of thermally evaporated iron phthalocyanine (FePc) organic thin films as a function of growth temperature and postdeposition *in situ* annealing time. A bilayer model was necessary to refine the FePc XRD data. Results using this model provide clear evidence that the first molecular layer of FePc contacting the sapphire substrate differs from the subsequent uniformly spaced molecular layers, indicating a Stranski-Krastanov growth mode. The  $\alpha$ -to- $\beta$  structural phase transformation of FePc was observed as a function of substrate temperature. No significant effect of postdeposition *in situ* annealing time was observed. Atomic force microscopy (AFM) measurements reveal a temperature-dependent morphology as the FePc changes from grains, to extended films, and finally shows crystallite formation for increasing deposition temperature. Structural characteristics obtained by SUPREX refinement and AFM quantitatively agree for surface roughness and average molecular layer spacing.

DOI: 10.1103/PhysRevB.72.104113

PACS number(s): 61.66.Hq, 81.15.Hi, 68.55.Jk, 68.37.-d

### I. INTRODUCTION

Many physical properties depend strongly on structural properties such as crystallinity, roughness, and strain. Structural characterization is thus a prerequisite to understanding and unlocking the potentially interesting physical properties of materials. X-ray diffraction (XRD) is a well-known technique for structural characterization. SUPREX is a general procedure for the quantitative structural refinement of superlattice structures and thin films.<sup>1-5</sup> It employs a general kinematic diffraction model that includes both average atomic structure and structural disorder for refining measured x-ray diffraction profiles. A nonlinear fitting algorithm is applied, with which structure parameters are iteratively adjusted to minimize the disagreement between the data and model calculations. SUPREX has been successfully implemented in many thin film systems, including magnetic multilayers,<sup>6</sup> crystalline/amorphous multilayers,<sup>7</sup> and layered high- $T_c$  superconductors.<sup>8,9</sup> Because scattered x-ray intensity is measured, the phase information is lost and it is thus impossible to directly convert the intensities to obtain the structure of a material. By fitting the measured XRD intensity profiles with model calculations, it is possible to obtain the structure. This type of structural characterization is commonly used in XRD and neutron diffraction from bulk powder samples using the Rietveld refinement procedure.<sup>10</sup> With this method, the structure of a single unit cell is modeled. The relative intensities of diffraction peaks are determined from the structure factor of the unit cell, and line profiles are fit to a structurally independent profile shape function. In contrast, the SUPREX refinement procedure for thin films uses the relative intensities *and* line profiles to determine the average unit cell and deviations from this average.

In this paper we present the first application of the SUPREX thin film refinement of XRD to organic molecular beam epitaxy (OMBE) deposited organic thin films in order to obtain quantitative structural information that is otherwise inaccessible. In particular, we studied thermally evaporated iron phthalocyanine (FePc,  $\text{Pc}=\text{C}_{32}\text{H}_{16}\text{N}_8$ ) films that were

nominally ten molecular layers thick. Though we focus only on FePc, we have successfully applied this refinement to CuPc and CoPc. Due to the general nature of the theoretical formalism, the refinement can be extended to all organic thin films.

The metallophthalocyanines (MPc) are a family of planar organic molecules with one metal atom located in the molecule's center.<sup>11</sup> Bulk crystals of MPcs grow in high aspect ratio needles, which is a macroscopic expression of their highly anisotropic molecular structure; molecule-molecule interactions are greatest when the platelike molecules are face-to-face rather than side-to-side. Such an affinity leads to stacking where the metal atoms form one-dimensional (1D) chains, strong intrachain and weak interchain coupling between metal atoms exists, and highly anisotropic optical, electrical, and magnetic properties result.<sup>12-14</sup> In general, MPcs are robust molecular compounds that sublime at relatively low temperatures and are thus readily deposited using OMBE techniques. They have been observed in many crystalline polymorphs, though the most readily studied by OMBE are the  $\alpha$  and  $\beta$  phases.<sup>15</sup> The bulk lattice parameters ( $\mathbf{a}, \mathbf{b}, \mathbf{c}, \beta$ ) from powder diffraction of orthorhombic  $\alpha$ -FePc and monoclinic  $\beta$ -FePc are (25.5, 3.79, 25.2 Å, 90.0°) and (14.61, 4.80, 19.41 Å, 120.8°), respectively<sup>16</sup> (Fig. 1). MPcs have been studied by a myriad of techniques on many different substrates.<sup>17-30</sup> Their semiconducting and optical properties have motivated several studies of MPc-based devices such as organic light emitting diodes,<sup>31</sup> photovoltaics,<sup>32</sup> field-effect transistors,<sup>33</sup> and sensors,<sup>34</sup> but they are also of general interest for optoelectronics,<sup>35</sup> organic electronics,<sup>36</sup> and magnetism.<sup>14,37-39</sup>

The information typically obtained by  $\theta$ - $2\theta$  x-ray diffraction studies that utilize modeling is limited to electron density, thickness, and roughness of organic thin film materials.<sup>40-44</sup> In contrast, the SUPREX thin film refinement can obtain quantitative information about all of these plus detailed structural information such as lattice spacing along the momentum transfer direction, average number of atomic

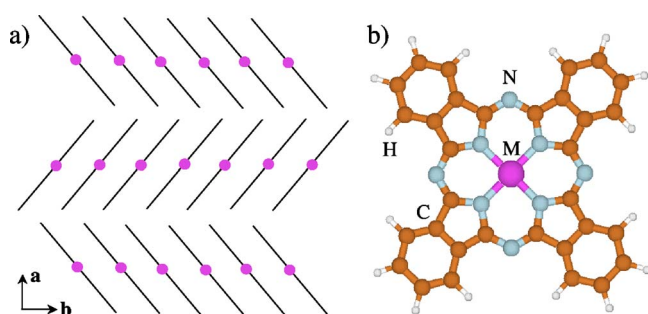


FIG. 1. (Color online) (a) Schematic of metallophthalocyanine crystal structure. The **a** and **b** directions are perpendicular and parallel to the substrate surface in our work. (b) Metallophthalocyanine ( $\text{MC}_{32}\text{H}_{16}\text{N}_8$ ) molecule.

layers, strain, and interdiffusion, and is flexible enough to model both simple and complex systems. It is our hope that this paper will initiate detailed quantitative structural studies of thin film organic materials by XRD. This technique is now applicable to organic thin films because the quality of these systems has improved drastically in recent years. In particular, high quality films [those exhibiting finite size effects or molecular layering by XRD and atomic force microscopy (AFM) measurements, respectively] that are ripe for SUPREX refinement have been observed in perylene derivatives,<sup>43–45</sup> pentacene,<sup>46</sup> hexaphenyl,<sup>47</sup> and lead phthalocyanine.<sup>21</sup>

## II. EXPERIMENTAL DETAILS

Commercial FePc was sequentially purified via sublimation in a vacuum furnace at  $\sim 10^{-3}$  Torr and 300 °C three times prior to insertion into the OMBE chamber. A low temperature effusion cell was used with an alumina crucible to deposit FePc onto  $\text{Al}_2\text{O}_3$  (11 $\bar{2}$ 0) at an average rate of 0.2 Å/s at a deposition pressure of  $1.2 \times 10^{-7}$  Torr. The substrates were ultrasonically cleaned in acetone, then methanol, blown dry with nitrogen gas, and then inserted into the chamber within minutes of cleaning. All films were grown to a nominal thickness of ten monolayers, as monitored by a calibrated quartz crystal microbalance. Substrates were held at constant deposition temperatures of 30, 100, 200, 225, and 250 °C, and postdeposition *in situ* annealing at the same temperature was performed for 0, 1, 2, 4, and 8 additional h. All samples were kept under a vacuum of  $\sim 100$  mTorr unless they were being measured. XRD measurements were performed using a Rigaku RU-200B diffractometer.  $\text{Cu } K_\alpha$  radiation was filtered with a curved graphite single crystal monochromator. The incident beam was collimated by two 0.5° slits between the x-ray source and sample. The momentum resolution was defined by two 0.3 mm slits between the sample and the detector. The sample was aligned perpendicular to the momentum transfer direction and coupled  $\theta$ - $2\theta$  scans were performed at 0.06° per minute. AFM measurements were performed in tapping mode using a Multimode AFM with a Nanoscope IV controller. Veeco silicon cantilevers with resonant frequencies of  $\sim 270$  kHz were used. All measurements were performed under ambient conditions.

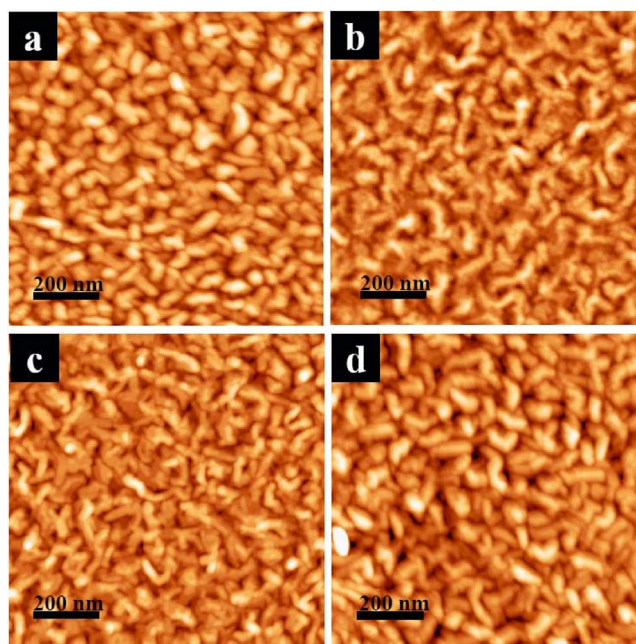


FIG. 2. (Color online) Four FePc films grown and *in situ* annealed at 100 °C for (a) 0, (b) 2, (c) 4, and (d) 8 h. Postdeposition *in situ* annealing had no significant effect on the structure of the films for any growth temperature. The images presented are representative of the morphology observed in different locations on the films.

## III. RESULTS

We observed no systematic or significant change in XRD, SUPREX refinement results, or AFM data for samples annealed at the deposition temperature for any time up to 8 h, for any deposition temperature. Figure 2 shows samples prepared at 100 °C with 0, 2, 4, and 8 h of postdeposition *in situ* annealing at the growth temperature. It is important to note that only a single diffraction peak (100), including higher orders up to (800), was observed for all films studied, indicating well ordered films. The intensities of the higher order peaks increased with deposition temperature, but were also found to be independent of postdeposition *in situ* annealing. The results and uncertainties we report for a given deposition temperature were therefore obtained by averaging over all anneal times.

The SUPREX refinement parameters available for crystalline layers include the average number of atomic layers ( $N$ ), the roughness ( $\sigma$ ), the lattice spacing ( $d$ ), lattice deviations (i.e., strain) near the substrate ( $\Delta d_1$ ) and vacuum ( $\Delta d_2$ ) interfaces, and an exponential length scale ( $\alpha$ ) over which the lattice deviations occur. For multilayer films, an interface between two layers is characterized by its thickness  $a$ , and its roughness  $c$ . These are the typical parameters used to describe multilayer films, though depending on the specific system, some such as the strain parameters are not always necessary. In those cases, the unnecessary parameters are removed from the model so as to avoid erroneous refinement results due to excessive parameters. Fixed material-specific parameters are entered for each layer, including the in-plane atomic density, the Debye-Waller coefficient, the atomic

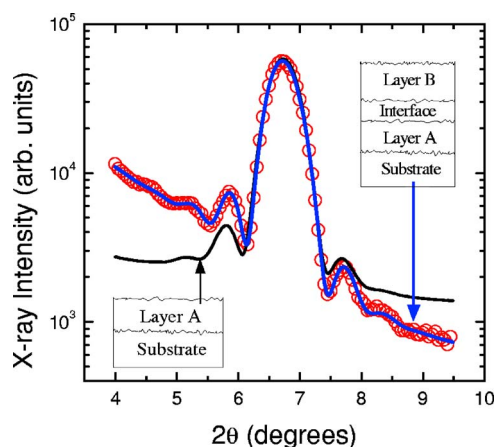


FIG. 3. (Color online)  $\theta$ - $2\theta$  XRD profile around the (100) peak of a  $\sim 10$  ML FePc film (open symbols) with SUPREX refinement using a single layer model and a bilayer model. The two models are shown schematically.

scattering power, and dispersion corrections. As a first order approximation, we assume that the scattering from FePc molecules is dominated by the single metal atom because of the large atomic number difference, and hence scattering power, between it and the other constituent atoms. To this end, all input parameters were those of the metal; the in-plane atomic density was adjusted in accord with known FePc lattice parameters. Though we presently have the luxury of making this assumption, SUPREX is not confined to organic materials containing metal atoms. Specialized models have been successfully developed and implemented in the past for complex multi-atomic structures (e.g.,  $Y_1Ba_2Cu_3O_7$ -based superlattices),<sup>9</sup> so the future development of a model for specific organic thin films is possible.

We began refining XRD data using a single layer crystalline film model. However, this model could not be used to accurately refine any of the data. The model was redefined to include an initial crystalline layer in contact with the substrate (layer A), a top crystalline layer (layer B), and an interfacial layer between A and B. The parameters for each layer will be denoted by appropriate subscripts (e.g., the  $d$  spacing of layer B is  $d_B$ ). To illustrate the need to expand to this bilayer model, Fig. 3 shows the measured XRD profile around the (100) peak of a typical FePc thin film compared to the best results of the two models. Note that a correction for the sloping background is included in both models to refine the raw data. The bilayer model is clearly superior. A third model that instead added an amorphous layer between the substrate and crystalline layer could not reproduce the data with physically acceptable parameters.

The oscillations about the central diffraction peak in Fig. 3 are called finite size effects, and are due to the small film thickness. Here, the films were ten molecular layers (ML), which is  $\sim 140$  Å. These oscillations are caused by coherent x-ray scattering from the entire sample, and their existence indicates a high degree of thickness uniformity. Finite size effects are not observed for films with extensive roughness or global thickness variations. Information about film roughness and strain near the film interfaces can be obtained by

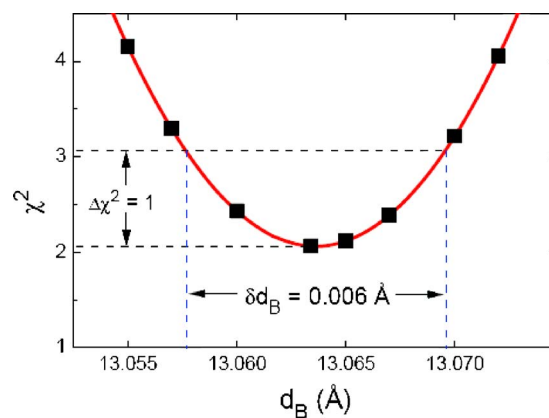


FIG. 4. (Color online) Example  $\chi^2$  study and uncertainty estimate. The parabolic shape indicates the parameter  $d_B$  has been minimized. The uncertainty is estimated by the change in  $d_B$  that increases  $\chi^2$  by unity. For this example,  $d_B = 13.063 \pm 0.003$  Å.

refining XRD data containing finite size effects. As previously noted, the improvement of OMBE techniques has led to the observation of finite size effects in several different organic thin films; the quantitative refinement described here can be extended to such systems.

The average  $\chi^2$  value of all fittings performed on all samples using the bilayer model was 2.6 with a standard deviation of 1.2. Due to the complexity of the model and the number of parameters involved, numerous local minima (and hence erroneous results) may exist on the multidimensional  $\chi^2$  surface. We verified that global minima were obtained by studying  $\chi^2$  as a function of each of the refinement parameters. Additionally, we used these studies to estimate the uncertainty associated with each parameter; the uncertainty of parameter  $n$  is defined generally as the perturbation of  $n$  that increases  $\chi^2$  by unity.<sup>48</sup> An example study of  $\chi^2$  as a function of  $d_B$  for one FePc thin film is shown in Fig. 4. The uncertainty associated with each refinement parameter proved to be universally smaller (by an order of magnitude in some cases) than the reproducibility associated with the film growth. These uncertainties are likely underestimates because evaluating uncertainty in this manner tacitly assumes uncorrelated parameters, which is not necessarily the case for all of the parameters we consider. For this reason, all uncertainties quoted henceforth regard sample-to-sample variations, not the  $\chi^2$ -based fitting uncertainties described here; as previously noted, the results and uncertainties for a given deposition temperature were obtained by averaging over all anneal times.

Figure 5 summarizes SUPREX refinement results as a function of deposition temperature. Within experimental error, the interface thickness  $a$ , number of monolayers of layer A ( $N_A$ ), and  $d_A$  were all found to be temperature independent. The A-B interface was  $\sim 5$  Å. Interestingly, we found that layer A was universally one molecular layer, with an associated  $d_A$  of  $\sim 10$  Å. Layer B was found to have  $N_B \sim 9$  ML, and  $d_B$  exhibited a systematic temperature dependence, decreasing from 13.25 Å at 100 °C to 12.90 Å at 250 °C. This shift of  $d_B$  shows the  $\alpha$ -to- $\beta$  structural phase transformation, and has been studied previously.<sup>15,19,25</sup>



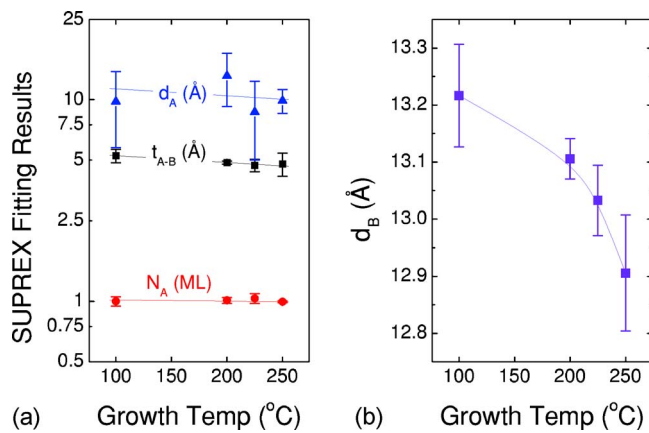


FIG. 5. (Color online) SUPREX refinement results using a bilayer model as a function of deposition temperature. The lines are guides to the eye. (a) Number of monolayers of layer A ( $N_A$ ),  $d$  spacing of layer A ( $d_A$ ), and A-B interface thickness ( $t_{A-B}$ ). (b)  $d$  spacing of layer B showing  $\alpha$ -to- $\beta$  structural phase transformation.

Strain was incorporated into the bilayer model by allowing the  $d$ -spacing of layer B to vary as  $d_B + \Delta d_{B1}$ ,  $d_B + \Delta d_{B1}e^{-\alpha}$ , and  $d_B + \Delta d_{B1}e^{-2\alpha}$  for the first three molecular layers near the A-B interface, and as  $d_B + \Delta d_{B2}e^{-2\alpha}$ ,  $d_B + \Delta d_{B2}e^{-\alpha}$ , and  $d_B + \Delta d_{B2}$  for the three layers near the vacuum interface; all other layers retain  $d_B$ . In all cases, including strain decreased  $\chi^2$  by an insignificant amount. It is not clear whether the improvement of the fittings using strain was due to the actual existence of strain in the films, or the near doubling of the number of available fitting parameters. We thus conclude that the strain in layer B (all but the first molecular layer) of the FePc films is negligible. In conjunction with the necessity of adopting a bilayer model to fit the XRD data and the observation that  $N_A = 1$ , these results suggest that layer A serves as a strain relief layer. This is reminiscent of Stranski-Krastanov growth.<sup>49</sup>

Figure 6 shows SUPREX results for  $\sigma_B$  normalized to  $N_B$  as a function of growth temperature with supporting AFM images. As shown in Fig. 6(a), SUPREX refinement results quantitatively agree with AFM-based roughness measurements. The roughness parameter is defined as the width of a Gaussian describing a distribution of discrete thickness fluctuations over the entire sample, where “discrete” means that the thickness varies by an integer number of molecular planes. Since we observe only a single diffraction peak and its higher orders for all samples, this is a reasonable approach. Because  $\theta$ - $2\theta$  XRD is only sensitive to the  $z$  coordinate (perpendicular to the substrate), these measurements cannot determine whether or not these fluctuations are correlated laterally into islands, as the AFM images indicate. It is important to note that these roughness values are not an error bar for the number of layers, but rather represent fluctuations of the number of layers at the vacuum-film interface. Another way to interpret this roughness is as a description of how the occupation of the layers decreases toward the vacuum side of the film, specifically fit to a Gaussian centered at the average film thickness.

The XRD profiles for the films grown at ambient temperatures showed no finite size oscillations about the (100) dif-

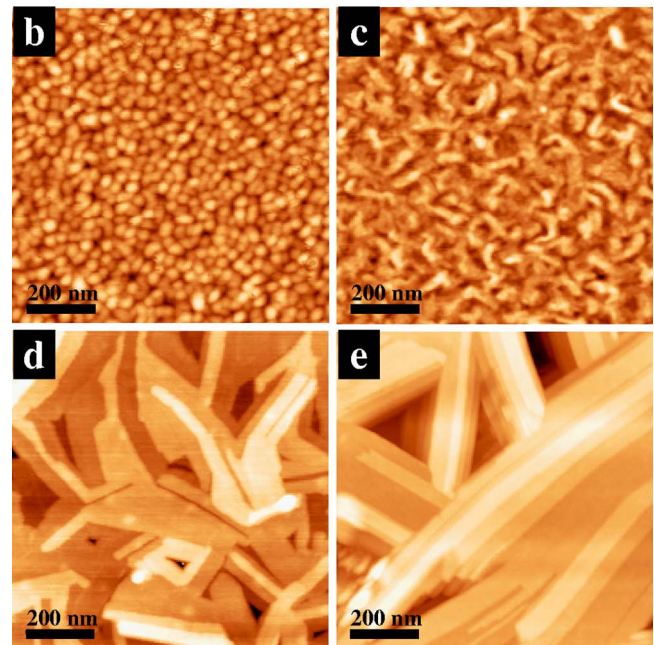
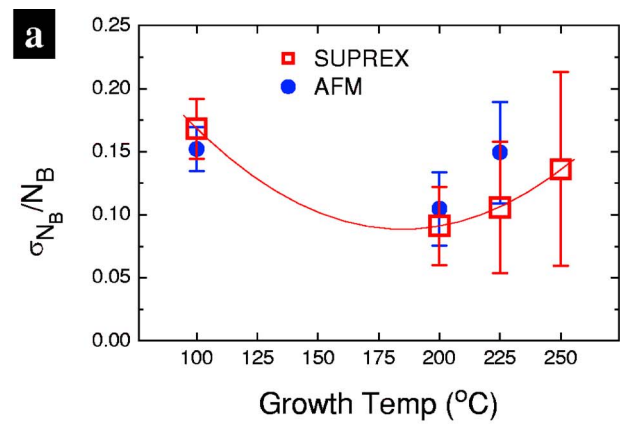


FIG. 6. (Color online) (a) Roughness of layer B normalized to the thickness of layer B. The line is a guide to the eye. Increased size and density of pinholes made defining roughness from AFM measurements difficult for 225 °C, leading to the large error bars. Similarly, roughness measurements were not meaningful for films grown at 250 °C, and have been excluded. AFM images of  $\sim 10$  ML FePc films grown on sapphire at substrate temperatures of (b) 30, (c) 100, (d) 200, and (e) 250 °C. The images presented are representative of the morphology observed in different locations on the films.

fraction peak, and were thus too low in quality to be refined. For ambient and 100 °C growth temperatures we observe similar films with dense granular formations [Figs. 6(b) and 6(c)] and AFM-measured rms roughness values of 1.2 ML ( $\sim 15$  Å). For depositions at 200 °C we observe extended flat regions with low pinhole densities and no globally preferred in-plane growth direction [Fig. 6(d)]. On a local scale, however, these films have a preferred growth direction. Samples grown at 225 °C show similar flat regions to the 200 °C films, but with increased roughness. For 250 °C films [Fig. 6(e)] it is apparent that the FePc is beginning to evolve from a film to crystallites. We observed many regions on 250 °C samples where crystallites vertically protruded from the sur-

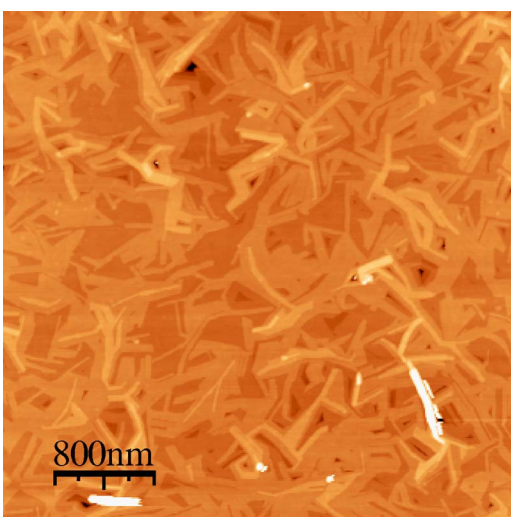


FIG. 7. (Color online)  $4\ \mu\text{m} \times 4\ \mu\text{m}$  AFM image of FePc grown at  $200\ ^\circ\text{C}$ . Each differently shaded region corresponds to an individual molecular layer. SUPREX refinement results show that FePc films grown at this temperature have a roughness of  $0.8 \pm 0.2$  ML. These films also show a minimum pinhole density.

face, resulting in increased pinhole density and size. The temperature at which the FePc starts to grow as crystallites rather than films may thus be slightly above  $225\ ^\circ\text{C}$ . This would explain the low average roughness with larger variations for  $225\ ^\circ\text{C}$  films, while by  $250\ ^\circ\text{C}$  crystallite formation is exhibited. This behavior has been seen in many cases where we presume the MPc purity or surface preparation (or lack thereof) significantly altered the relative magnitudes of the substrate-molecule and intermolecular interactions so that the formation of extended crystals occurred at low temperatures.<sup>17,26,50</sup>

We observe films of unique quality for FePc grown at  $200\ ^\circ\text{C}$ . The roughness of these films found using SUPREX was  $0.8 \pm 0.2$  ML. The low density of pinholes in these FePc films can be seen in the  $4\ \mu\text{m} \times 4\ \mu\text{m}$  AFM image shown in Fig. 7, and Fig. 8 shows a line section through a pinhole in one of these films. The observed steps correspond to  $\sim 13\ \text{\AA}$ , which quantitatively agrees with the SUPREX refinement results for the molecular layer spacing. The AFM-measured roughness restricted to a single molecular layer was at the noise level of the microscope ( $\sim 2\ \text{\AA}$ ). Each different shade in these images corresponds to a single molecular layer. A similar observation was recently made for PbPc,<sup>21</sup> though for those films the molecular terraces were confined to islands, not extended over large areas as we observe here.

#### IV. CONCLUSIONS

The SUPREX refinement procedure has been demonstrated for high quality OMBE-deposited FePc organic thin

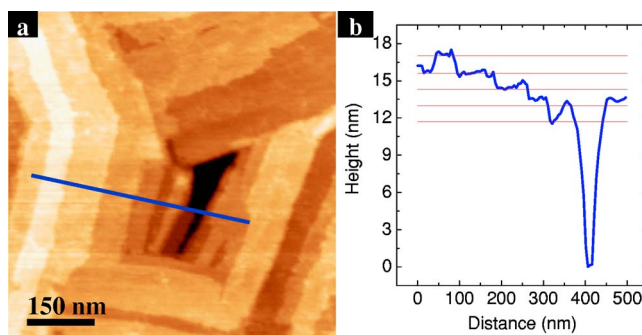


FIG. 8. (Color online) (a) AFM image showing the molecular layers near a pinhole in an FePc film grown at  $200\ ^\circ\text{C}$ . (b) Height profile along the solid line. The horizontal lines correspond to  $13\ \text{\AA}$  molecular layers, which quantitatively agrees with SUPREX refinement results. The pinhole extends through the film down to the substrate.

films. A bilayer thin film model was required in order to accurately refine XRD data. Refinement results indicate a single crystalline FePc molecular layer with an associated  $d$  spacing of  $\sim 10\ \text{\AA}$  was formed at the film-substrate interface, separated from the rest of the crystalline film by an interfacial region of  $\sim 5\ \text{\AA}$ ; these results were independent of the deposition temperature. The remaining nine molecular layers of the film had a larger, uniform  $d$  spacing that was temperature dependent. We conclude that FePc grows in the Stranski-Krastanov growth mode on  $(11\bar{2}0)$  sapphire, with the initial molecular layer serving as a strain relief layer. We found no significant structural dependence on postdeposition *in situ* annealing for times up to 8 h when annealed at the deposition temperature. The  $\alpha$ -to- $\beta$  structural phase transformation of FePc was observed as the  $d$  spacing shifted from  $13.25$  to  $12.90\ \text{\AA}$  as the deposition temperature was changed from  $100$  to  $250\ ^\circ\text{C}$ . AFM imaging revealed a growth transition with granular films below  $200\ ^\circ\text{C}$ , flat extended films with distinct individual molecular layering for  $200$ – $225\ ^\circ\text{C}$ , and the onset of crystallite formation at  $250\ ^\circ\text{C}$ . SUPREX refinement results and independent AFM measurements quantitatively agree for film roughness and molecular layer spacing. This work shows that the SUPREX thin film refinement procedure can be successfully used for the structural characterization of organic thin films.

#### ACKNOWLEDGMENTS

This work was supported by an Air Force Office of Scientific Research MURI, and the California Institute for Telecommunications and Information Technology, Cal(IT)<sup>2</sup>.

- <sup>1</sup>E. E. Fullerton, I. K. Schuller, H. Vanderstraeten, and Y. Bruynseraede, *Phys. Rev. B* **45**, 9292 (1992).
- <sup>2</sup>I. K. Schuller, *Phys. Rev. Lett.* **44**, 1597 (1980).
- <sup>3</sup>W. Sevenhans, M. Gijs, Y. Bruynseraede, H. Homma, and I. K. Schuller, *Phys. Rev. B* **34**, R5955 (1986).
- <sup>4</sup>D. M. Kelly, E. E. Fullerton, J. Santamaria, and I. K. Schuller, *Scr. Metall. Mater.* **33**, 1603 (1995).
- <sup>5</sup>SUPREX is a free software package that can be obtained from [ischuller.ucsd.edu](http://ischuller.ucsd.edu).
- <sup>6</sup>I. K. Schuller, S. Kim, and C. Leighton, *J. Magn. Magn. Mater.* **200**, 571 (1999).
- <sup>7</sup>D. Neerincx, H. Vanderstraeten, L. Stockman, J.-P. Locquet, Y. Bruynseraede, and I. K. Schuller, *J. Phys.: Condens. Matter* **2**, 4111 (1990).
- <sup>8</sup>J. Guimpel, E. E. Fullerton, O. Nakamura, and I. K. Schuller, *J. Phys.: Condens. Matter* **5**, A383 (1993).
- <sup>9</sup>I. K. Schuller and Y. Bruynseraede, *Nanostruct. Mater.* **1**, 387 (1992).
- <sup>10</sup>H. M. Rietveld, *J. Appl. Crystallogr.* **2**, 65 (1969).
- <sup>11</sup>F. H. Moser and A. L. Thomas, *The Phthalocyanines* (CRC Press, Boca Raton, 1983).
- <sup>12</sup>E. Barrera, J. O. Osso, F. Schreiber, M. Garriga, M. I. Alonso, and H. Dosch, *J. Mater. Res.* **19**, 2061 (2004).
- <sup>13</sup>M. Ofuji, K. Ishikawa, H. Takezoe, K. Inhaba, and K. Omote, *Appl. Phys. Lett.* **86**, 062114 (2005).
- <sup>14</sup>S. Lee, M. Yudkowsky, W. P. Halperin, M. Y. Ogawa, and B. Hoffman, *Phys. Rev. B* **35**, 5003 (1987).
- <sup>15</sup>S. Yim, S. Heutz, and T. S. Jones, *J. Appl. Phys.* **91**, 3632 (2002).
- <sup>16</sup>JCPDS, *International Center for Diffraction Data, PC-PDF WIN V. 1.30* (International Center for Diffraction Data, Swarthmore, 1997).
- <sup>17</sup>S. Tabuchi, H. Tabata, and T. Kawai, *Surf. Sci.* **571**, 117 (2004).
- <sup>18</sup>Y.-L. Lee, W.-C. Tsai, C.-H. Chang, and Y.-M. Yang, *Appl. Surf. Sci.* **172**, 191 (2001).
- <sup>19</sup>L. Ottaviano, L. Lozzi, A. R. Phani, A. Ciattoni, S. Santucci, and S. D. Nardo, *Appl. Surf. Sci.* **136**, 81 (1998).
- <sup>20</sup>A. Miyamoto, K. Nichogi, A. Taomoto, T. Nambu, and M. Murakami, *Thin Solid Films* **256**, 64 (1995).
- <sup>21</sup>J. E. S. Kim, E. Lim, K. Lee, D. Cha, and B. Friedman, *Appl. Surf. Sci.* **205**, 274 (2003).
- <sup>22</sup>S. Tokito, J. Sakata, and Y. Taga, *Thin Solid Films* **256**, 182 (1995).
- <sup>23</sup>M. Nakamura, T. Matsunobe, and H. Tokumoto, *J. Appl. Phys.* **89**, 7860 (2001).
- <sup>24</sup>I. Chizhov, G. Scoles, and A. Kahn, *Langmuir* **16**, 4358 (2000).
- <sup>25</sup>O. Berger, W.-J. Fischer, B. Adolphi, S. Tierbach, V. Melev, and J. Schreiber, *J. Mater. Sci.: Mater. Electron.* **11**, 331 (2000).
- <sup>26</sup>M. Nakamura, Y. Morita, Y. Mori, A. Ishitani, and H. Tokumoto, *J. Vac. Sci. Technol. B* **14**, 1109 (1996).
- <sup>27</sup>H. Piesert, T. Schwieger, J. M. Auerhammer, M. Knupfer, M. S. Golden, and J. Fink, *J. Appl. Phys.* **90**, 466 (2001).
- <sup>28</sup>D. A. Evans, H. J. Steiner, S. Evans, R. Middleton, S. P. T. S. Jones, T. U. Kampen, D. R. T. Zahn, G. Cabailh, and I. T. McGovern, *J. Phys.: Condens. Matter* **15**, S2729 (2003).
- <sup>29</sup>M. Ofuji, K. Inaba, K. Omote, H. Hoshi, Y. Takamishi, K. Ishikawa, and H. Takezoe, *Jpn. J. Appl. Phys., Part 1* **41**, 5467 (2002).
- <sup>30</sup>T. S. Ellis, K. T. Park, S. L. Hulbert, M. D. Ulrich, and J. E. Rowe, *J. Appl. Phys.* **95**, 982 (2004).
- <sup>31</sup>T. Mori, T. Mitsuoka, M. Ishii, H. Fujikawa, and Y. Taga, *Appl. Phys. Lett.* **80**, 3895 (2002).
- <sup>32</sup>S. Senthilarasu, S. Velumani, R. Sathyamoorthy, A. Subbarayan, J. A. Ascencio, G. Canizal, P. J. Sebastian, J. A. Chavez, and R. Perez, *Appl. Phys. A* **77**, 383 (2003).
- <sup>33</sup>R. Zeis, T. Siegrist, and C. Kloc, *Appl. Phys. Lett.* **86**, 022103 (2005).
- <sup>34</sup>J. D. Wright, *Surf. Sci.* **31**, 1 (1989).
- <sup>35</sup>A. Yamashita and T. Hayashi, *Adv. Mater. (Weinheim, Ger.)* **8**, 791 (1996).
- <sup>36</sup>G. Witte and C. Wöll, *J. Mater. Res.* **19**, 1889 (2004).
- <sup>37</sup>A. B. P. Lever, *J. Chem. Soc.* **1965**, 1821 (1965).
- <sup>38</sup>M. Evangelisti, J. Bartolomé, L. J. de Jongh, and G. Filoti, *Phys. Rev. B* **66**, 144410 (2002).
- <sup>39</sup>K. Awaga and Y. Maruyama, *Phys. Rev. B* **44**, 2589 (1991).
- <sup>40</sup>M. Tolan, *X-Ray Scattering from Soft-Matter Thin Films* (Springer, Berlin, 1999).
- <sup>41</sup>D. Q. Li, M. Lutt, M. R. Fitzsimmons, R. Synowicki, M. E. Hawley, and G. W. Brown, *J. Am. Chem. Soc.* **120**, 8797 (1998).
- <sup>42</sup>M. Lutt, M. R. Fitzsimmons, and D. Li, *J. Phys. Chem. B* **102**, 400 (1998).
- <sup>43</sup>A. C. Dürr, F. Schreiber, M. Münch, N. Karl, B. Krause, V. Kruppa, and H. Dosch, *Appl. Phys. Lett.* **81**, 2276 (2002).
- <sup>44</sup>A. C. Dürr, F. Schreiber, K. A. Ritley, V. Kruppa, J. Krug, H. Dosch, and B. Struth, *Phys. Rev. Lett.* **90**, 016104 (2003).
- <sup>45</sup>B. Krause, A. C. Dürr, F. Schreiber, H. Dosch, and O. H. Seeck, *Surf. Sci.* **572**, 385 (2004).
- <sup>46</sup>R. Ruiz, D. Choudhary, B. Nickel, T. Toccoli, K.-C. Chang, A. C. Mayer, P. Clancy, J. M. Blakely, R. L. Headrick, S. Iannotta, G. G. Malliaras, *Chem. Mater.* **16**, 4497 (2004).
- <sup>47</sup>R. Resel, *Thin Solid Films* **433**, 1 (2003).
- <sup>48</sup>P. R. Bevington and D. K. Robinson, *Data Reduction and Error Analysis for the Physical Sciences*, 2nd ed. (McGraw-Hill, New York, 1992).
- <sup>49</sup>J. W. Matthews, *Epitaxial Growth Part B* (Academic Press, London, 1975).
- <sup>50</sup>K. Xiao, Y. Liu, G. Yu, and D. Zhu, *Appl. Phys. A* **77**, 367 (2003).